Spring 2016

A cost benefit analysis of SST based volt-var control

Guruprasad Ramani

A COST BENEFIT ANALYSIS OF SST BASED VOLT-VAR CONTROL

by

GURUPRASAD RAMANI

A THESIS

Presented to the Faculty of the Graduate School of the

MISSOURI UNIVERSITY OF SCIENCE AND TECHNOLOGY

In Partial Fulfillment of the Requirements for the Degree

MASTER OF SCIENCE

in

ELECTRICAL ENGINEERING

2016

Approved by
Mariesa L. Crow, Advisor
Jhi Young Joo
Shamsi Pourya

ABSTRACT

The overall objective is to perform a cost benefit analysis of the solid-state-transformer (SST)-based volt-var control (VVC). Two methods to improve the system power quality, or volt-var solutions are explored: a) achieving a unity power factor at all the load buses, and b) improving the system voltage profile to meet a desired voltage regulation requirement of $0.95<V_{bus}<1.05$ p.u. at all the buses of the distribution test system, for a given annual load profile. The test simulation is performed using the Open-DSS (Open-Distribution System Simulator) software on an IEEE-34 bus and its extended meshed test bed system. A cost benefit analysis of the proposed VVC solutions compares the relative annual cost advantages of implementing these solutions with respect to the base case system. The base case system is the original IEEE-34 radial and the extended meshed system without any compensation devices like capacitor banks, voltage regulators etc. and without the proposed VVC implemented.

ACKNOWLEDGMENTS

This research thesis has been made possible through the help and support of all my teachers, and my mother. First and foremost, I would like to thank Dr. Mariesa L. Crow, for her patience, mentorship, support and guidance throughout the course of the project. Without her mentorship, this research work would not have been possible.

Second, I would like to thank the other two members of the committee, Dr. Pourya Shamsi and Dr. Jhi-Young Joo, who have kindly accepted my request to be panelists for the thesis defense, and have agreed to review my thesis and provide their valuable feedback.

Third, I would like to thank all the professors at Missouri S&T, especially Dr. Mariesa Crow, Dr. Mehdi Ferdowsi, Dr. Jonathan Kimball, Dr. Kelvin T. Erickson, and Mr. Paul Nauert who are an inspiration to me and from whom I have learnt and acquired knowledge and skillsets for life. I am thankful to them as they have dedicated their lives to active research and have imparted their invaluable knowledge to me, which they gained through years of experience and study.

Finally, I would like to thank and acknowledge my mother, who has always stood by me and supported all my decisions. She has motivated me in all my pursuits in life, and to think and act independently and own my decisions.

TABLE OF CONTENTS

LIST OF FIGURES

LIST OF TABLES

Table Page

NOMENCLATURE

VVC – Volt-VAR Control

SSTs – Solid State Transformers

p.u. – Per Unit

UPF – Unity Power Factor

Base Case – The original IEEE-34 mesh extended test bed system without SSTs

NERC – North American Electrical Reliability Corporation

ERCOT – Electric Reliability Council of Texas

PQ – Power Quality

1. INTRODUCTION TO SOLID STATE TRANSFORMERS

1.1. SOLID STATE TRANSFORMERS

Transformers are electrical equipment used to transform the field voltage or current from one level to another in power networks. They are composed of steel or iron cores, and copper or aluminum coils. They contain mineral oil, which can serve as both a coolant and a dielectric medium. However, solid state transformers (SSTs) are not the same as the traditional transformers. Therefore the term SST is somewhat a misnomer. A solid state transformer is new type of power electronic transformer, which can be made coil free, self-regulating, and can also be used to correct power quality problems in power systems. They are also somewhat insensitive to harmonics and can prevent harmonic propagation in the power system. Moreover, there can be a significant reduction in individual size and weight of transformers with equivalent ratings. The basic structure of a solid state transformer is depicted in Figure 1.1 [11]:

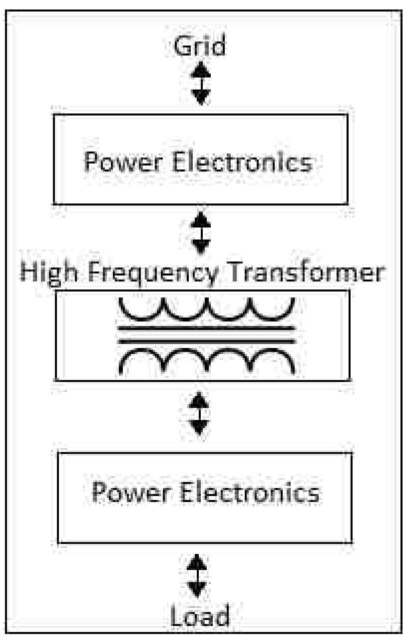

Figure 1.1: Basic structure of a solid state transformer [11]

The SST converts the grid voltage into a high AC frequency voltage. Similarly, the voltage is converted to the power frequency voltage through power electronics on the secondary side of the high frequency transformer, to obtain the load side low voltage [11].

Until recently, solid state transformers were deemed impractical for use in utility power applications due to the power limitations of the semiconductor materials. However, these limitations have been overcome with the development of SiC semiconductor switches [7]. Thus, the use of solid state transformers in modern power networks can radically change the way power is distributed in power systems by providing active control via power electronics [11].

1.2. POWER QUALITY IN POWER SYSTEMS

Power quality is an important concern in modern power systems. This is mainly due to the diverse nature of loads, such as adjustable speed drives (ASD) and power electronic equipment, information technology equipment like computers, printers, laptops, energy efficient lighting, and PLCs, which may cause degradation of line power. Due to the nonlinear nature of these loads, voltage waveform distortion frequently occurs. The availability of good quality power is critical to industrial, commercial, and residential customers. Some of the crucial sectors are the continuous process industry and the IT industry. A power disturbance in either of these sectors can have financial implications through loss of productivity and competitiveness. Some of these consumers require a higher level of power quality than is provided in modern electrical power networks, requiring the need for measures to be taken to achieve a higher power quality level. With NERC requirements for voltage limits on transmission systems and for maintaining high a power factor at load buses, it has become essential to study how a higher level of power quality can be achieved in power systems using modern technology such as SSTs [10].

1.3. THE IEEE-34 RADIAL TEST BED SETUP

Figure 1.2 shows a diagram of the IEEE-34 bus radial distribution test bed system. This system, as well as an extended meshed version, will be used to validate the proposed VVC. Subsequently, simulations on the extended meshed test bed system would be performed. The data for the test system are summarized in Tables 1.1 through 1.7.

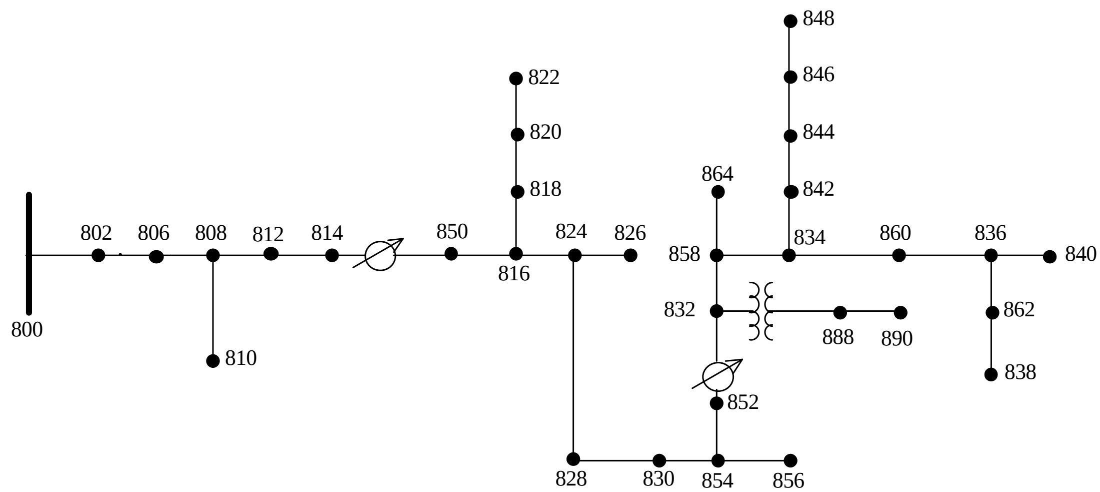

Figure 1.2: The IEEE-34 bus radial test bed distribution system [6]

Table 1.1 Overhead line configurations [6]

Config.	Phasing	Phase	Neutral	Spacing ID
		ACSR	ACSR	
300	B A C N	1/0	1/0	500
301	B A C N	#2 6/1	#2 6/1	500
302	A N	#4 6/1	#4 6/1	510
303	B N	#4 6/1	#4 6/1	510
304	B N	#2 6/1	#2 6/1	510

Table 1.2 Line data for IEEE-34 radial system [6]

Line Segment Data			
Node A	Node B	Length(ft.)	Config.
800	802	2580	300
802	806	1730	300
806	808	32230	300
808	810	5804	303
808	812	37500	300
812	814	29730	300
814	850	10	301
816	818	1710	302
816	824	10210	301
818	820	48150	302
820	822	13740	302
824	826	3030	303
824	828	840	301
828	830	20440	301
830	854	520	301
832	858	4900	301
832	888	0	XFM-1
834	860	2020	301
834	842	280	301
836	840	860	301
836	862	280	301
842	844	1350	301
844	846	3640	301
846	848	530	301
850	816	310	301
852	832	10	301
854	856	23330	303
854	852	36830	301
858	864	1620	302
858	834	5830	301
860	836	2680	301
862	838	4860	304
888	890	10560	300

Table 1.3 Shunt capacitors data for IEEE-34 radial system [6]

Node			
	Ph-A	Ph-B	Ph-C
844	kVAr	kVAr	kVAr
848	100	100	100
Total	150	150	150

Table 1.4 Distributed load data for IEEE-34 radial system [6]

Distributed Loads								
Node	Node	Load	Ph-1	Ph-1	Ph-2	Ph-2	Ph-3	Ph-3
A	B	Model	kW	kVAr	kW	kVAr	kW	kVAr
802	806	Y-PQ	0	0	30	15	25	14
808	810	Y-I	0	0	16	8	0	0
818	820	Y-Z	34	17	0	0	0	0
820	822	Y-PQ	135	70	0	0	0	0
816	824	D-I	0	0	5	2	0	0
824	826	Y-I	0	0	40	20	0	0
824	828	Y-PQ	0	0	0	0	4	2
828	830	Y-PQ	7	3	0	0	0	0
854	856	Y-PQ	0	0	4	2	0	0
832	858	D-Z	7	3	2	1	6	3
858	864	Y-PQ	2	1	0	0	0	0
858	834	D-PQ	4	2	15	8	13	7
834	860	D-Z	16	8	20	10	110	55
860	836	D-PQ	30	15	10	6	42	22
836	840	D-I	18	9	22	11	0	0
862	838	Y-PQ	0	0	28	14	0	0
842	844	Y-PQ	9	5	0	0	0	0
844	846	Y-PQ	0	0	25	12	20	11
846	848	Y-PQ	0	0	23	11	0	0
Total			262	133	240	120	220	114

Table 1.5 Spot load data for IEEE-34 radial system [6]

Spot Loads							
Node	Load	Ph-1	Ph-1	Ph-2	Ph-2	Ph-3	Ph-4
	Model	kW	kVAr	kW	kVAr	kW	kVAr
860	Y-PQ	20	16	20	16	20	16
840	Y-I	9	7	9	7	9	7
844	Y-Z	135	105	135	105	135	105
848	D-PQ	20	16	20	16	20	16
890	D-I	150	75	150	75	150	75
830	D-Z	10	5	10	5	25	10
Total		344	224	344	224	359	229

Table 1.6 Transformer data for IEEE-34 radial system [6]

Transformer Data					
	kVA	kV-high	kV-low	R - %	X - %
Substation:	2500	69 - D	24.9 -Gr. W	1	8
XFM -1	500	24.9 - Gr.W	4.16 - Gr. W	1.9	4.08

Table 1.7 Regulator data for IEEE-34 radial system [6]

Regulator Data			
Regulator ID:	1		
Line Segment:	814 - 850		
Location:	814		
Phases:	A - B -C		
Connection:	3-Ph,LG		
Monitoring Phase:	A-B-C		
Bandwidth:	2.0 volts		
PT Ratio:	120		
Primary CT Rating:	100		
Compensator Settings:	Ph-A	Ph-B	Ph-C
R - Setting:	2.7	2.7	2.7
X - Setting:	1.6	1.6	1.6
Volltage Level:	122	122	122
Regulator ID:	2		
Line Segment:	852 - 832		
Location:	852		
Phases:	A - B -C		
Connection:	3-Ph,LG		
Monitoring Phase:	A-B-C		
Bandwidth:	2.0 volts		
PT Ratio:	120		
Primary CT Rating:	100		
Compensator Settings:	Ph-A	Ph-B	Ph-C
R - Setting:	2.5	2.5	2.5
X - Setting:	1.5	1.5	1.5
Volltage Level:	124	124	124

1.4. EXTENSION OF THE RADIAL TEST SYSTEM TO A MESHED SYSTEM

Figure 1.3 shows a meshed system extension of the IEEE-34 radial bus test system. For the extended system, the load data are given in Table 1.8 while the line data are given in Table 1.

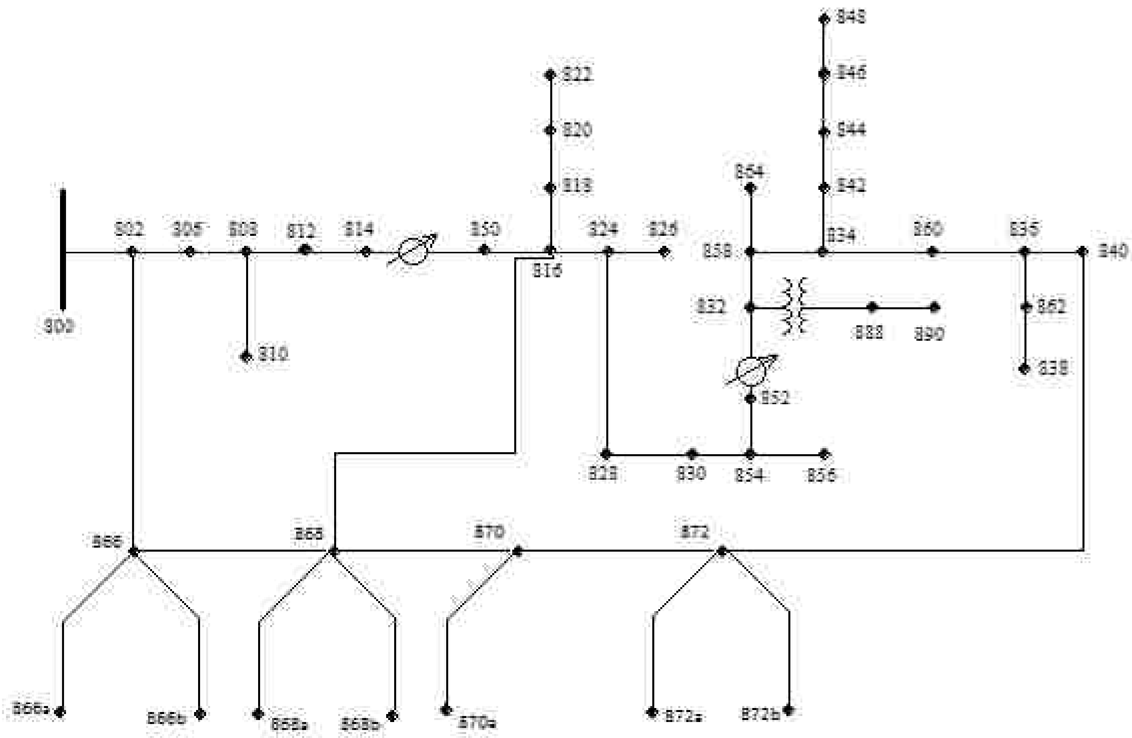

Figure 1.3: Meshed system extension of IEEE-34 radial test system

Table 1.8 Load data for extended meshed system

Spot Loads							
Node	Load	Ph-1	Ph-1	Ph-2	Ph-2	Ph-3	Ph-4
	Model	kW	kVAr	kW	kVAr	kW	kVAr
866a	Y-PQ	75	38	75	38	75	38
866b	Y-PQ	75	38	75	38	75	38
868a	Y-PQ	75	38	75	38	75	38
868b	Y-PQ	75	38	75	38	75	38
870a	Y-PQ	75	38	75	38	75	38
872a	Y-PQ	75	38	75	38	75	38
872b	Y-PQ	75	38	75	38	75	38
Total		375	190	375	190	375	190

Table 1.9 Line data for extended meshed system

Line Segment Data				
			Phase-A/B/C	
Node A	Node B	Length(mi.)	R(Ohms/mi)	X(Ohms/mi)
802	866	9	1.9156	1.3827
866	868	9	1.9156	1.3827
868	870	9	1.9156	1.3827
870	872	9	1.9156	1.3827
816	868	6	1.9156	1.3828
840	872	6	1.9156	1.3828
866	866a	0.2094	1.9156	5.65526
866	866b	0.1397	1.9156	5.65144
868	868a	0.1862	1.9156	5.6532
868	868b	0.1397	1.9156	1.3827
870	870a	0.1397	1.9156	5.65144
872	872a	0.2094	1.9156	5.65526
872	872b	0.1397	1.9156	5.65144

The resistance and reactance values of the conductors for each line in Ohms/mile are the same as shown above for each of the phases A, B, and C. The test system is implemented in the Open-DSS software.

2. THE OPEN-DSS SOFTWARE AND THE BASE-CASE SIMULATION

2.1. INTRODUCTION AND A BRIEF OVERVIEW OF THE OPEN-DSS SOFTWARE

The Open Distribution System Simulator (Open-DSS or simply DSS), is a simulation software platform for electrical power distribution systems. It is open source software, and it is available to the general public. It is available in both standalone versions (it can be run independently), or it can be driven by an external software such as MATLAB, Visual Basic, through its COM interface. Its executable version has a text based interface, with which users can develop/write scripts and view solutions. The software supports the RMS steady state or the frequency domain analysis usually performed for the planning and analysis of utility distribution systems. It also supports many types of analyses designed to support future needs with the advent of smart grids and utility level deregulations across the globe [8].

Many of the software's features were incorporated to meet the needs of distribution generation analyses. Its other features are harmonic analysis, smart grid applications and energy efficient analysis of smart grid applications [8].

Some applications of the Open-DSS software are to areas such as distribution planning and analysis, general multi-phase ac circuit analysis, analysis of distributed generation interconnections, annual load and generation simulations, risk-based distribution planning studies, probabilistic planning studies, solar PV system simulation, wind plant simulations, nuclear plant station auxiliary transformer modeling, distribution automation control assessment, protection system simulation, storage modeling, distribution feeder simulation with AMI data, distribution state estimation, ground voltage rise on transmission systems, geomagnetically-induced currents (GIC), EV impacts simulations, co-simulation of power and communications Networks, analysis of unusual transformer configurations, harmonic and inter-harmonic distortion analysis, neutral-to-earth voltage simulations, development of IEEE test feeder cases, phase shifter simulation, arc furnace simulation, impulse loads (car crushers, etc.) and more [8].

The software has many built-in solution modes, such as a) snapshot power flow, b) daily power flow, c) yearly power flow, d) harmonics, e) dynamics, f) fault study, and g) Monte Carlo fault studies [8].

A COM interface allows diverse users to perform different types of studies, providing flexibility and multiple diverse options. For example, it can be driven through MATLAB, C#, Python, R, or VBA of the Microsoft Office. Its various custom solution modes can be executed through the COM interface. The tool is equipped with excellent mathematical capabilities, as well as graphical user interface for viewing results. Users who need to repeatedly use a particular feature, can access it with built-in solution control module as well as the text base command interface [8].

The COM interface can be used to directly access the text-based command interface and the various methods and properties for accessing many of the Open-DSS's models. The input can be routed to a text file. The output results can be retrieved either through the COM based interface, or through various output files. Many output/export files are written in comma separated value (CSV) format which can be easily imported into tools such as Microsoft Excel, or MATLAB for further analysis and processing [8].

The structure of the Open-DSS software is as shown in Figure 2.1:

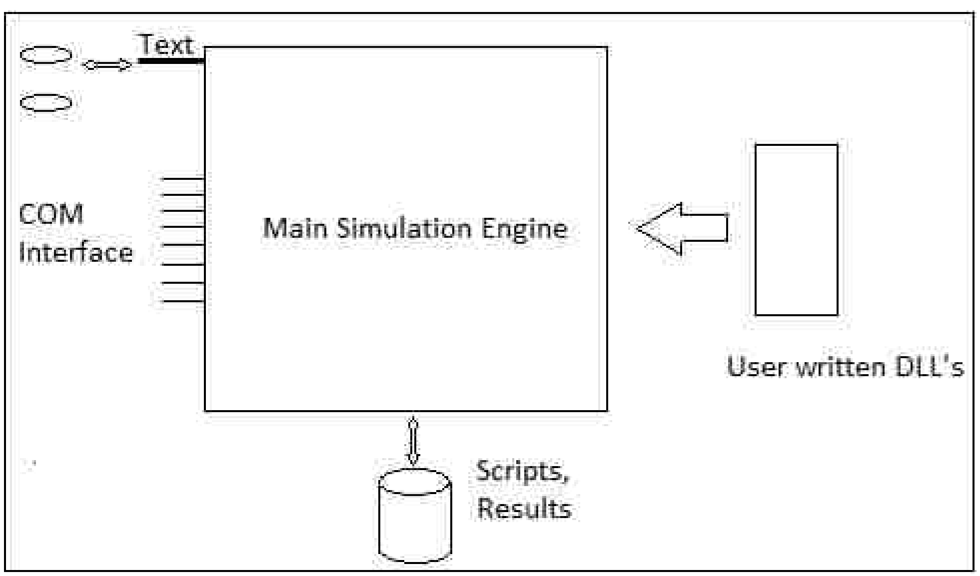

Figure 2.1: Open-DSS structure [8]

2.2. THE BASECASE SYSTEM SIMULATION IN OPEN-DSS

2.2.1. System Setup for Base Case Simulation in Open-DSS. The intention for the base-case scenario is to simulate the fully loaded IEEE-34 bus radial test system and the extended meshed test system in Open-DSS with all its loads, but without compensating devices, including capacitor banks and voltage regulators, which help to improve the system power factors and voltages. This procedure defines the worst case scenario, i.e. the worst voltages and power factors that would result from a fully loaded system. The base case analysis is based on the annual cumulative load data in the ERCOT (Electric Reliability Council of Texas) region for 2013 [9]. This data provides annual load data with hourly active and reactive power variations.

A base case was established a) on the IEEE-34 bus radial test system, and b) on the extended meshed test system. The inclusion of the meshed system is to verify the applicability of the proposed VVC on both meshed and radial systems.

For the system power quality solutions explored in the next chapter, the solid state transformers are used to inject VARs into the system dynamically at each hour when the load changes, unlike the static compensation devices which are traditionally installed to provide fixed VAR compensation at all time. This implementation of SSTs is compared to the base case to measure the performance of SSTs on the system without other VAR compensation devices. The cost differences between the base case and the SST case are then determined.

2.2.2. Explanation for Highest Active Power Losses and Lowest System Voltages. For the base case simulation, the active power consumed at each phase of the load bus is given by:

$$P = V * I * \cos(\phi) \quad (1)$$

where

P - Total active power consumption at the load bus in consideration

V - Voltage at the load bus

I - Current consumed by the load kW

$\cos(\phi)$ - Power factor at a given load bus

The reactive power consumed at each single phase load bus is determined by:

$$Q = V * I * \sin(\phi) \quad (2)$$

where

Q - Total reactive power consumption at the load bus in consideration

Due to the heavy loads being consumed at the load buses and to the voltage drop along the distribution feeder (due to the line resistances and reactances), the voltages at the end of the feeder may become unacceptably low. Also, since reactive power is being consumed at each load bus, the power factor of the load buses may be much less than unity. Since the active power being consumed at each load bus is fixed, then from equation (1), the currents drawn by the load bus from the substation will be obviously higher when there is significant reactive loading. These higher currents lead to higher system losses, and larger voltage drops along the distribution feeder.

2.2.3. Plots of Total Active Power Losses, Voltages at Selected Buses and Substation Power Factor Versus Time. Figure 2.2 shows the plots of the total active power losses versus time for the base case simulation for the meshed system. During hours of high load, the active and reactive power consumption is high at the load buses. This basically causes higher currents to be drawn from the substation. This means higher line losses during hours of peak load. Figures 2.3 through 2.6 show the plots of voltages at selected buses versus time. The higher currents cause higher line resistance and reactance drops, resulting in lower voltages at the load buses. Figure 2.7 shows the power factor of the entire system observed at the substation versus time for the base case scenario. It is observed that power factor value as low as 0.875 are reached at the substation during peak load hours. The results obtained from the base case scenario would be compared with the VVC solutions to illustrate the effectiveness of the control.

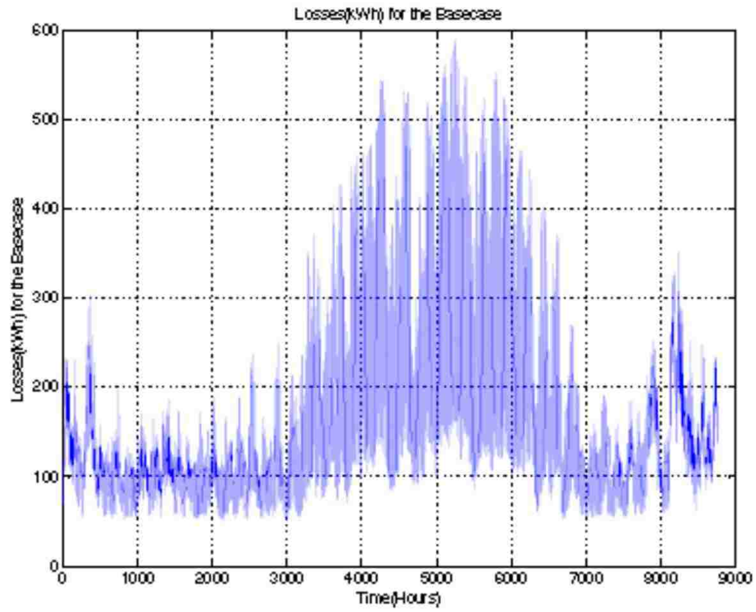

Figure 2.2: Total active power losses versus time, base case

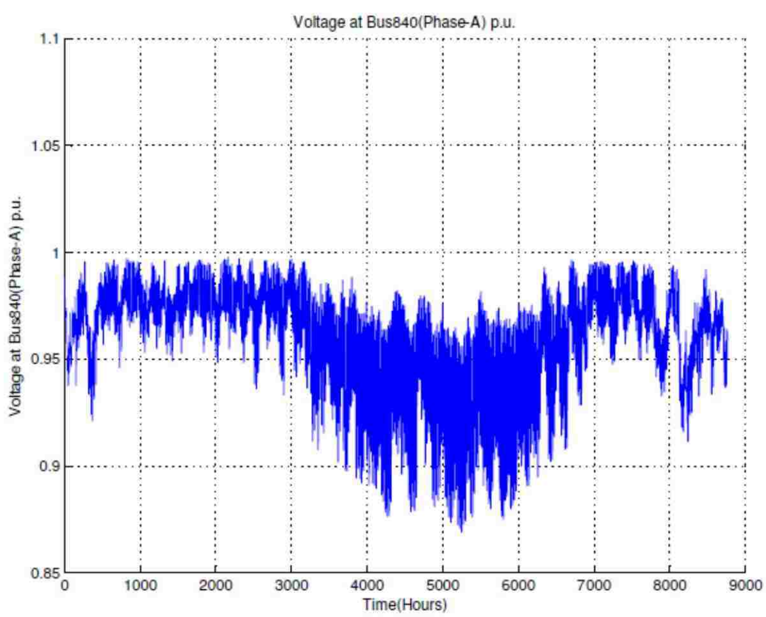

Figure 2.3: Voltage at bus 840, phase-A (p.u.), base case

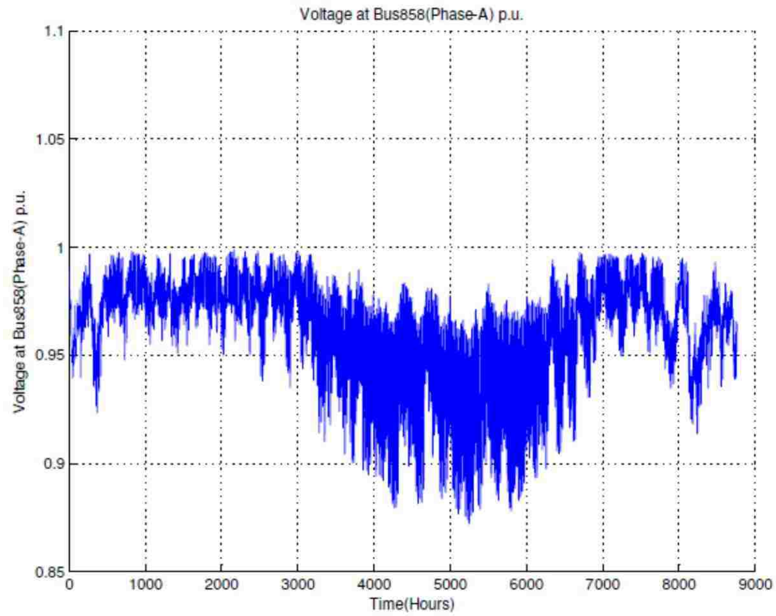

Figure 2.4: Voltage at bus 858, phase-A (p.u.), base case

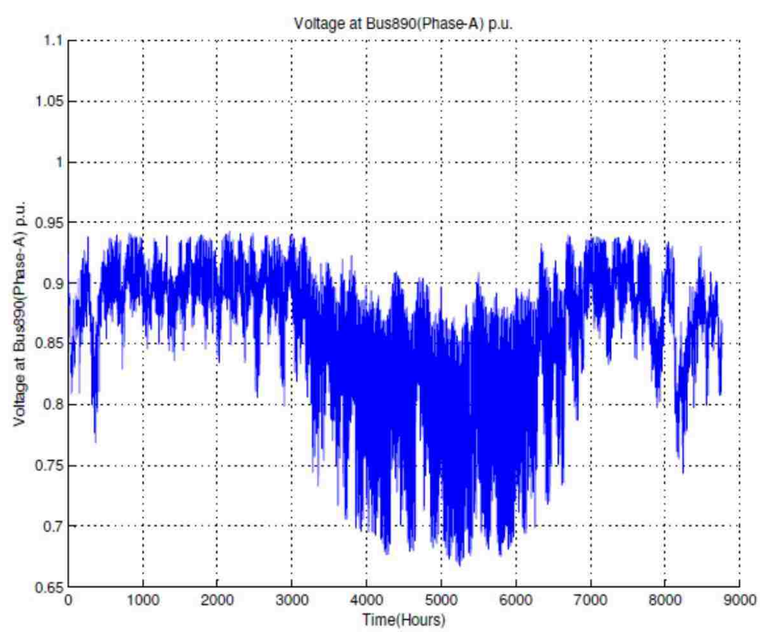

Figure 2.5: Voltage at bus 890, phase-A (p.u.), base case

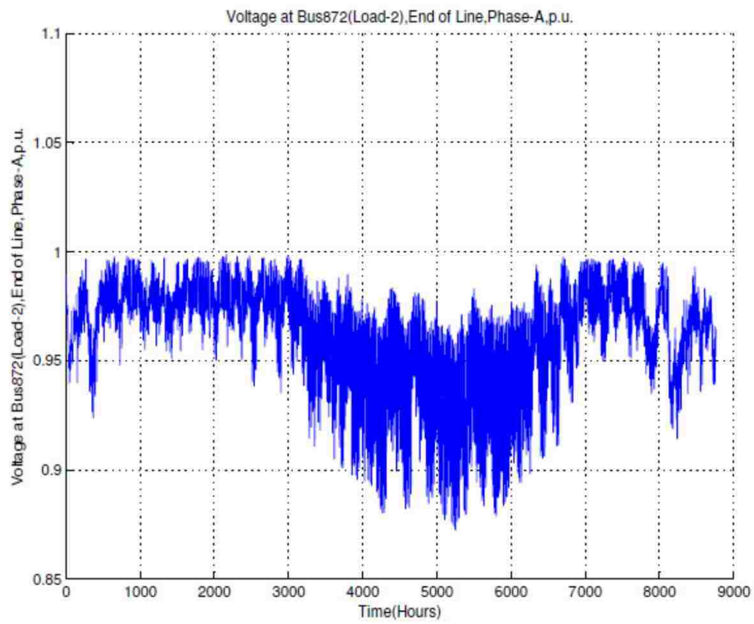

Figure 2.6: Voltage at bus 872 (Load-2, End of Line), phase-A (p.u.), base case

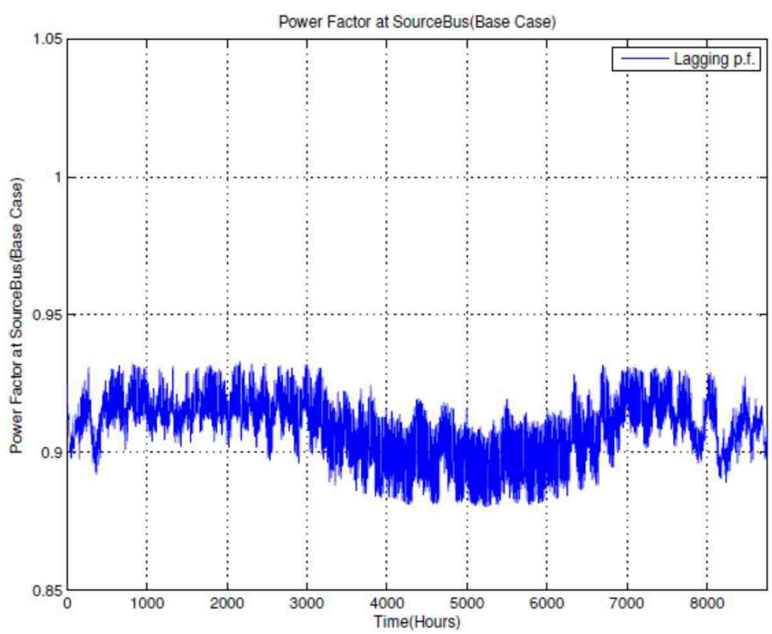

Figure 2.7: Power factor at the substation, base case

2.2.4. The Problem of Low Voltages. The system power losses for the base case are higher at each hour due to the reasons discussed in earlier section. Figures 2.3 through 2.6 capture the voltage profiles at selected load buses that result in the base case. It is to be noted that these voltages are unacceptably low only during peak load hours (when the current consumption is high which cause greater line voltage drops), but have healthy values during off-peak hours. Figure 2.7 captures the power factor at the substation, which becomes as low as 0.875 during peak load hours. A power factor below 0.9 p.u. lagging is considered low for a substation. It is desirable that power factors of 0.95 p.u. lagging and above are maintained at the substation level. These indicate power quality problems in the system, which need to be addressed through dynamic VAR compensation by SSTs.

3. VOLT-VAR CONTROL STRATEGIES

3.1. UNITY POWER FACTOR CONTROL CASE SCENARIO

The low power factors at distribution buses are corrected by installing SSTs at each load bus, to locally compensate the reactive power. This achieves unity power factor at each load bus.

3.1.1. System Setup for Achieving UPF at Each Load Bus. For the unity power factor (UPF) solution, as the load varies the reactive power consumed at each hour is sensed at the load bus, and is fed back to the dedicated SST. The SST then injects the same level of reactive power back into the system, maintaining unity power factor at load bus. This action is completed almost instantaneously (in the order of a few milliseconds).

3.1.2. Explanation for Lowest Active Power Losses and Improved System Voltages. The UPF approach has several advantages. Firstly, the total active power losses in the system are at their minimum.

For the unity power factor case scenario, the active power consumed in each phase of the load bus is given by the equation:

$$P = V * I \qquad (3)$$

where

P - Total active power consumption at the distribution bus in consideration

V - Voltage at the distribution bus

I - Current consumed by the load

Note the absence of the term $\cos(\phi)$ here, because at unity power factor, $\cos(\phi) = 1$. In the base case scenario, the majority of the system voltages were unacceptably low due to i) heavy loads at the distribution buses and ii) the magnitude of the voltage drop along the distribution feeder (due to the resistance and reactance of the lines). In contrast, in the unity power factor case scenario, the reactive power consumption at each distribution bus is locally compensated by SSTs, thus decreasing the current drawn by the loads and thereby reducing the voltage drop along the feeder.

3.1.3. Plots of Total Active Power Losses, Voltages at Selected Buses and Substation Power Factor Versus Time. Figure 3.1 shows the plot of the total active power losses versus time for the unity power factor case scenario obtained for the meshed system. Figures 3.2 through 3.5 show the voltages at selected buses versus time. Figure 3.6 shows the power factor at the substation versus time. The plot of power factor versus time indicates that near unity power factor at the substation. The power factor at the substation is not identically unity due to the slight reactive power losses in the feeder. Note, however that unity power factor is exactly achieved at each distribution bus due to local compensation of reactive VARs through the SSTs.

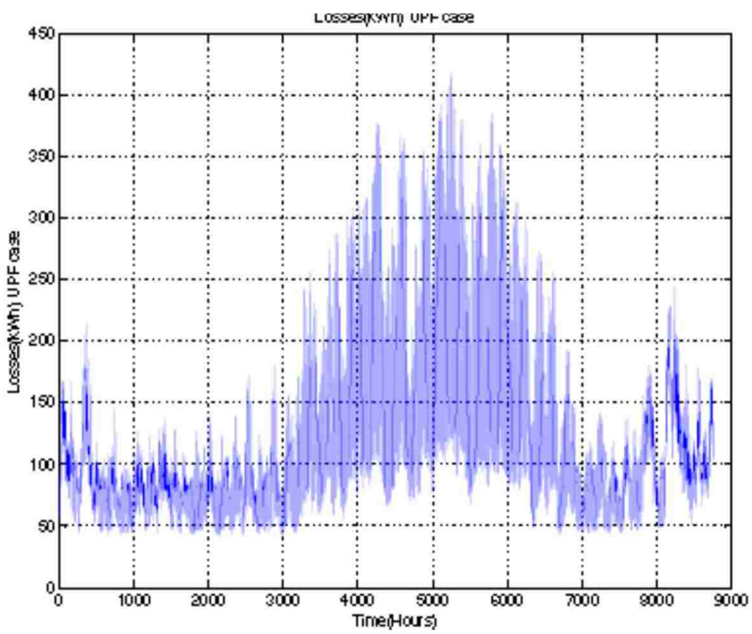

Figure 3.1: Total active power losses versus time, UPF case

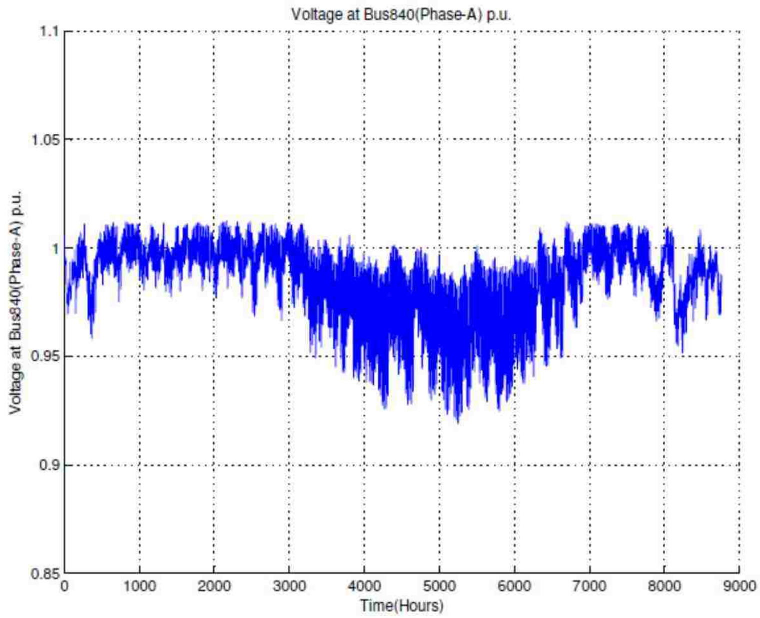

Figure 3.2: Voltage at bus 840, phase-A (p.u.), UPF case

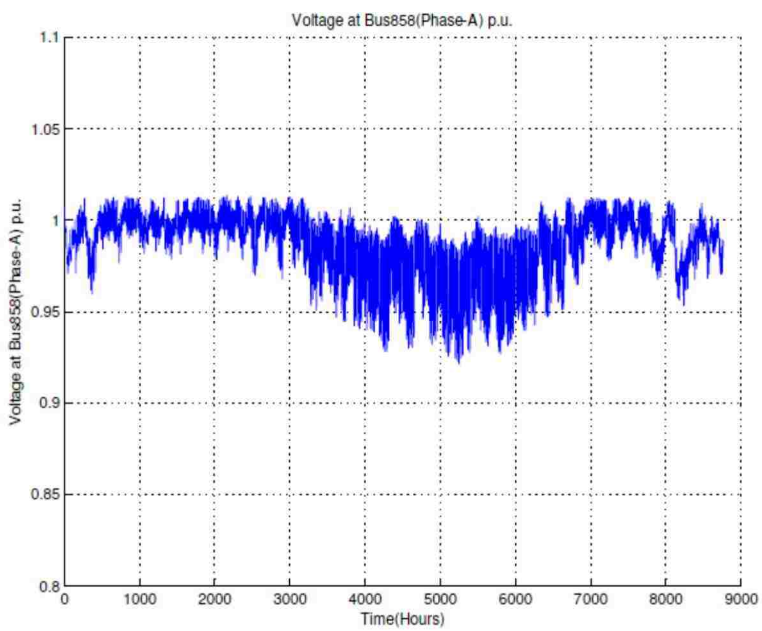

Figure 3.3: Voltage at bus 858, phase-A (p.u.), UPF case

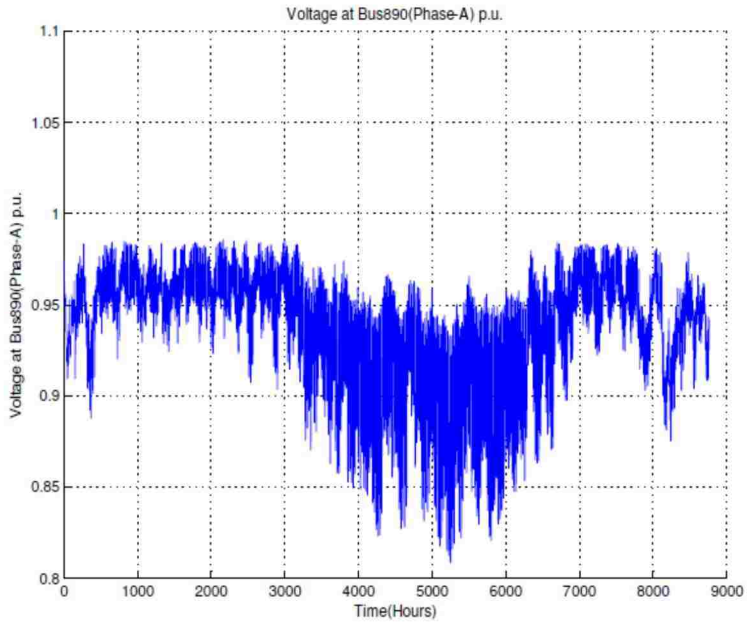

Figure 3.4: Voltage at bus 890, phase-A (p.u.), UPF case

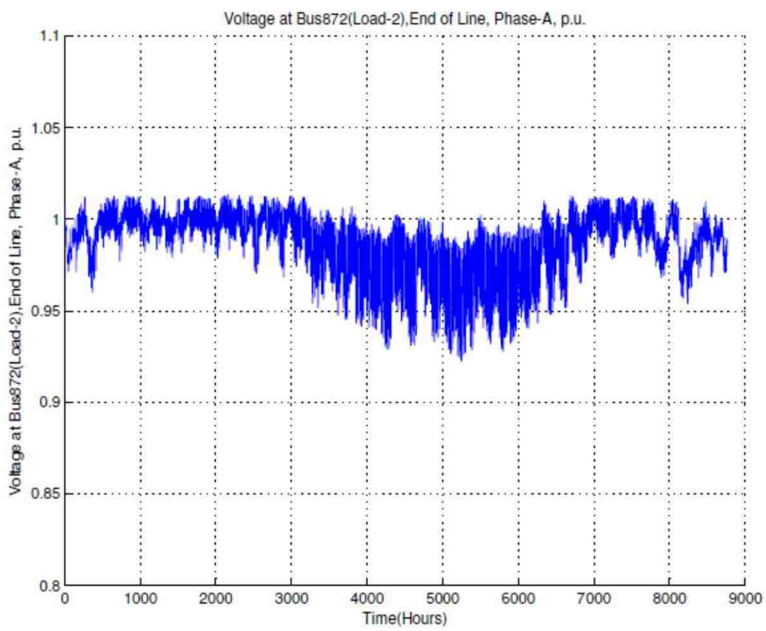

Figure 3.5: Voltage at bus 872 (Load-2, End of Line), Phase-A (p.u.), UPF case

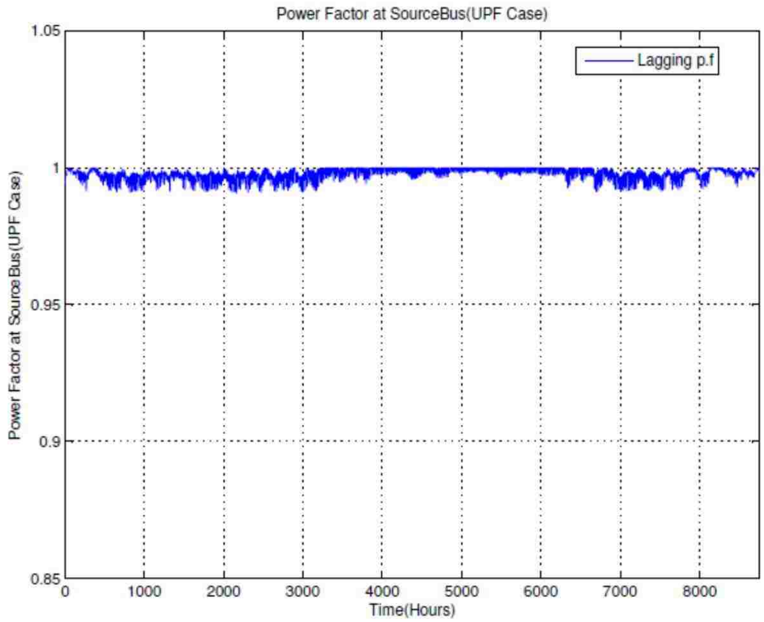

Figure 3.6: Power factor at the substation, UPF case

3.2. VOLTAGE REGULATION CONTROL CASE SCENARIO

While unity power factor control improves the bus voltages, there is no direct control of bus voltages and they may still become too high or too low depending on the bus load. The UPF control provides some improvement in the distribution bus voltages compared to the base case scenario. However, the voltage improvement is not always as desired, as it is not regulated within specified limits. Moreover, voltages below 0.9 p.u. are still considered undesirable, although they are not uncommon in distribution systems. The lowest voltages seen for the unity power factor case scenario are slightly above 0.8 p.u., which is a cause of concern. Therefore, a more advanced scheme using volt-var control (VVC) is required to maintain the bus voltages within a predetermined range.

3.2.1. System Setup for Voltage Regulation Control Case. The voltage improvement control algorithm aims to improve the system voltage through reactive power control. For this case, the system is assumed to be initially operating at unity power factor (through the use of dedicated load bus SSTs for the UPF case scenario). Thus, the voltage regulation control case is implemented over the UPF case scenario as a platform. Apart from the dedicated load bus SSTs installed in the system for achieving unity power factor, the three phase SSTs each at bus 840 and bus 890 are considered to be pilot buses in the control scheme. These SSTs are dedicated specifically for the voltage control action. The SSTs at the distribution buses dedicated for UPF control inject VARs into the system in response to changes in load, compensating for the load reactive power to maintain a unity power factor. A few seconds (30 seconds to a minute) after the load changes and the voltages stabilize, the pilot SSTs perform their VAR control action. A flow chart showing the pilot bus VVC is shown in Figure 3.7.

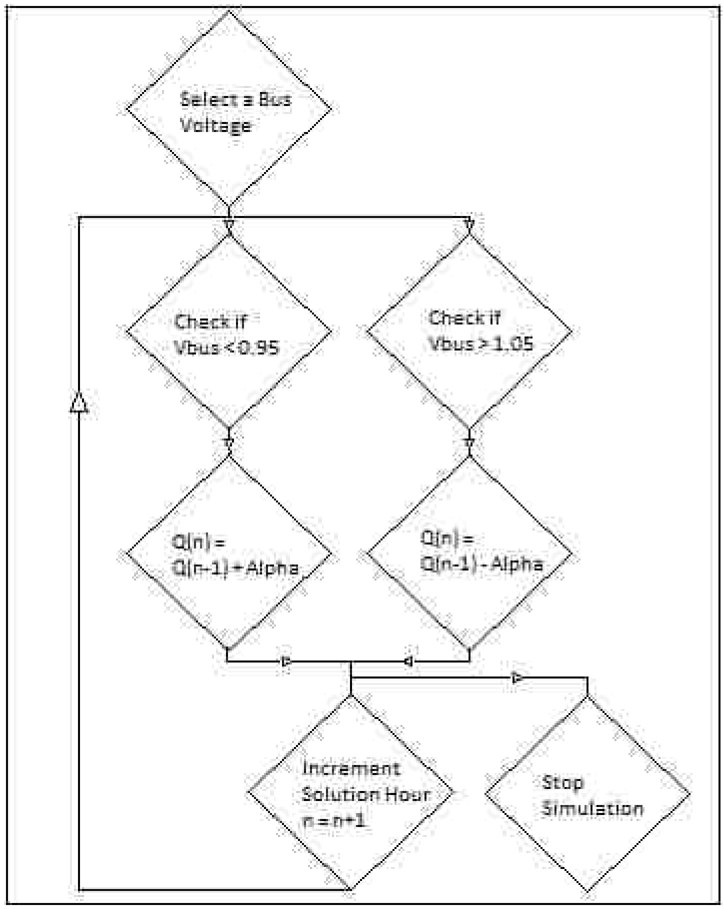

Figure 3.7: Flow chart for voltage regulation control algorithm [5]

where

$Q(n)$ - Reactive power injected into the system by a pilot SST at the nth hour

$Q(n-1)$ - Reactive power injected into the system at the $(n-1)th$ hour.

$Alpha$ – Fixed reactive power by which $Q(n-1)$ is incremented if voltage at the pilot bus exceeds 1.05 p.u., or decremented if voltage at the pilot bus falls below 0.95 p.u.

It is important to have the requisite time delay of 30 seconds to 1 minute between the UPF control and the voltage control to allow the bus voltages to stabilize before the voltage control action is implemented.

This system could be considered as a double feedback control system, analogous to current mode controlled power electronic dc-dc converters. The requisite time delay is analogous to the frequency bandwidth that is to be allowed between the voltage control action of the external loop and the current control action of the internal loop, necessary for proper control action.

It is evident from the flow chart that voltages at distribution buses are being controlled between the limits of 0.95 p.u. and 1.05 p.u. These limits are based on the NERC guidelines for transmission system voltages and are used as a reference for this test system. The voltages at bus 840 and bus 890 tend to drop to unacceptably low values in the base case and the unity power factor case scenarios, which justifies the selection of these buses for performing voltage control action. As a result of voltage control at these two buses, the voltages at other distribution buses are automatically regulated within the limits specified, as they have improved voltages than these two buses. Thus, the selection of these two buses for voltage regulation control is a reasonable choice.

The VARs produced by the pilot SSTs will be injected into the distribution feeder. Since the system is already operating at unity power factor before voltage control action, therefore the substation injects minimal reactive power into the system, to compensate for the reactive power losses in the lines.

After the voltage control action, there is excess of reactive power in the system injected by pilot SSTs which needs to be absorbed. These are absorbed at the substation, resulting in leading power factors at the substation. The VARs flowing from pilot bus SSTs to the substation take all the available paths, so that the circuit is completed. They do not flow into other radial nodes (buses) which are open circuit and do not lead to the substation. The reactive VARs help to directly improve the system voltages, determined by equation (2), which is repeated below:

$$Q = V * I * \sin(\phi)$$

Here, the reactive power injected by the pilot SST is in addition to the compensation provided by unity power factor control, which maintains

$$Q(bus) = 0 \tag{4}$$

At each load bus prior to voltage control action. After voltage control, there are positive VARs in the system.

The active power consumption is fixed at the load bus, however the reactive VARs injected are adjusted so that the desired voltage level is achieved, as per the flow chart in Figure 3.7. The power factor at each bus is obtained from the following equation

$$cos(\phi) = P/(P\text{^}2 + Q\text{^}2)^{0.5} \tag{5}$$

where

P - Active power consumed by load at the bus

Q – Reactive power available at the bus as a result of injection from pilot bus SST

The reactive power at many load buses is non-zero and may be positive, resulting in leading non-unity power factors. Figure 3.8 shows the plot of the total active power losses versus time. Since power factors at many distribution buses are less than unity, as per equation (1), the currents drawn from the substation are higher. This leads to higher losses as compared to the unity power factor control case. Figures 3.9 through 3.12 show the plot of voltages at selected buses vs time for the voltage control case scenario for the meshed system. The voltages at all the buses are well regulated and within the limits desired. Figure 3.13 shows the plot of the power factor at the substation versus time. As observed, the power factors at the substation are again non unity, but now due to excessive VARs in the system. Also, note that they are leading power factors.

3.2.2. Impact of the VVC on Active Power Losses. Since the VARs improve the system voltages at all distribution buses, the voltage profiles of these buses for the voltage control case are within their specified limits. But due to the increased VARs in the system, the power factor at many distribution buses become non-unity. The active power at a particular distribution bus is given in equation (1), which is repeated here:

$$P = V * I * \cos(\phi)$$

Although the voltage at each load distribution bus is improved, the power factor at the bus decreases. These two effects somewhat counterbalance each other, resulting in currents (drawn from substation) that are lower than the base case scenario, but higher than the UPF case scenario. As a result, the system active power losses are higher than the UPF case scenario but lower than the base case scenario. Figures 3.9 through 3.12 show the effect of the voltage control action. Note that the voltages are between the limits of 0.95 p.u. and 1.05 p.u. for both the radial and meshed test systems at all the distribution buses.

3.2.3. Plots of Total Active Power Losses, Voltages at Selected Buses and Substation Power Factor Versus Time. Figure 3.8 shows the plot of the total active power losses versus time for the unity power factor case scenario obtained for the meshed system. Figures 3.9 through 3.12 show the voltages at selected buses versus time. It is evident that the voltages at various distribution buses are well within specified limits. Figure 3.13 shows the power factor at the substation versus time. The plot indicates a non-unity leading power factor. Due to the non-unity power factor but improved bus voltages, the currents drawn from the substation by load buses are higher as compared to the UPF case but lower than base case. Consequently, the power losses are higher than the unity power factor case, but lower than the base case.

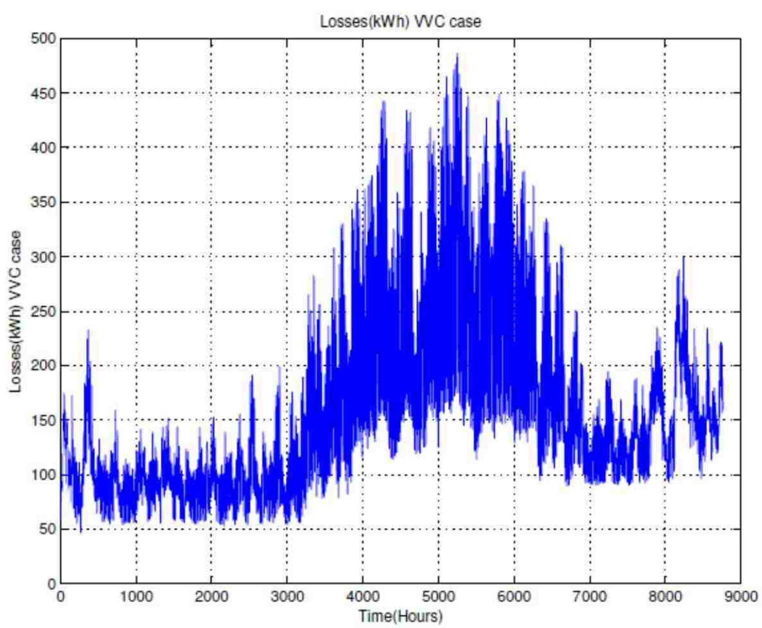

Figure 3.8: Total active power losses versus time, voltage regulation control case

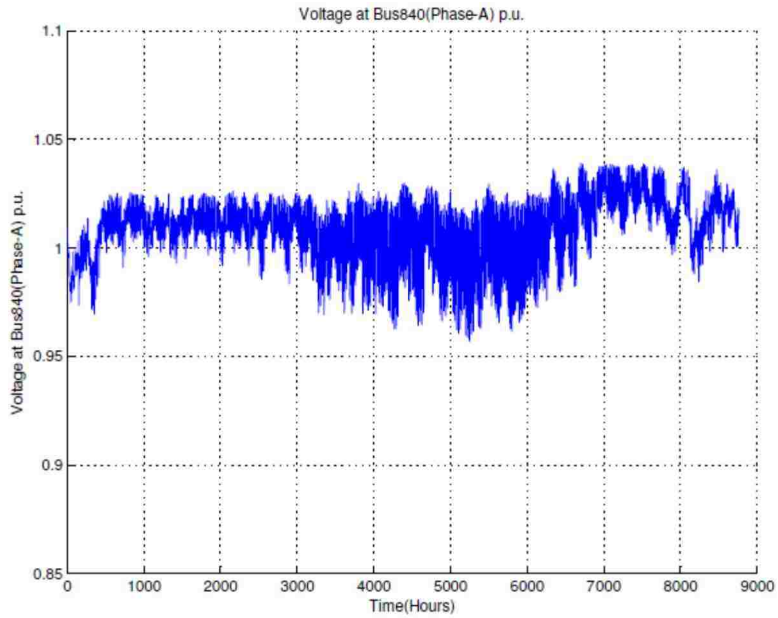

Figure 3.9: Voltage at bus 840, phase-A (p.u.), voltage regulation control case

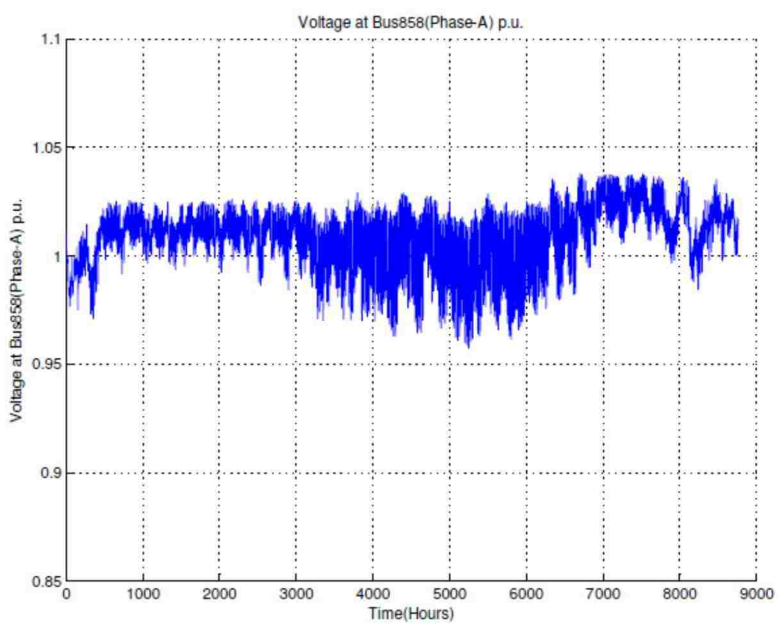

Figure 3.10: Voltage at bus 858, phase-A (p.u.), voltage regulation control case

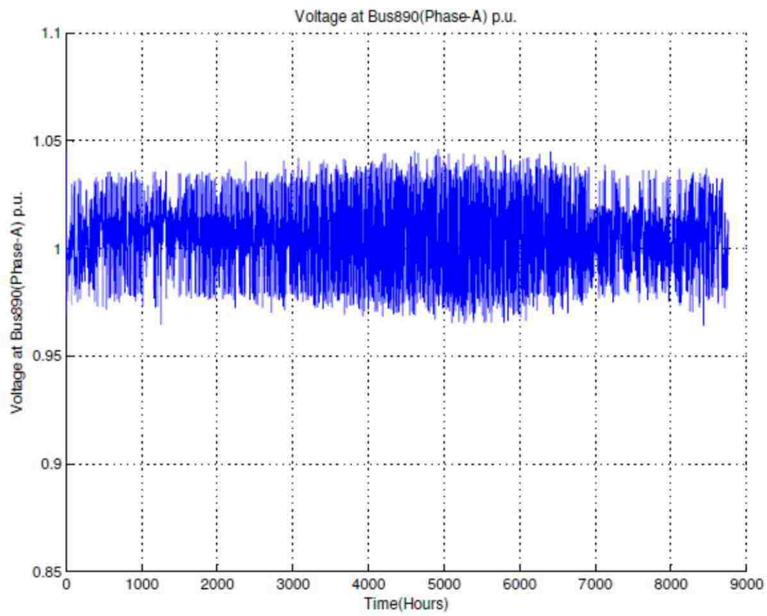

Figure 3.11: Voltage at bus 890, phase-A (p.u.), voltage regulation control case

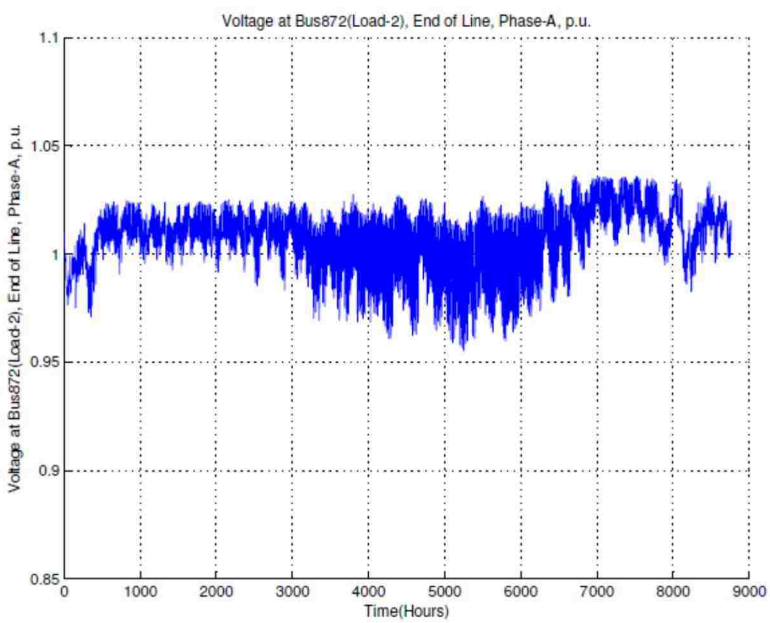

Figure 3.12: Voltage at bus 872 (Load-2, End of Line), phase-A (p.u.), voltage regulation control case

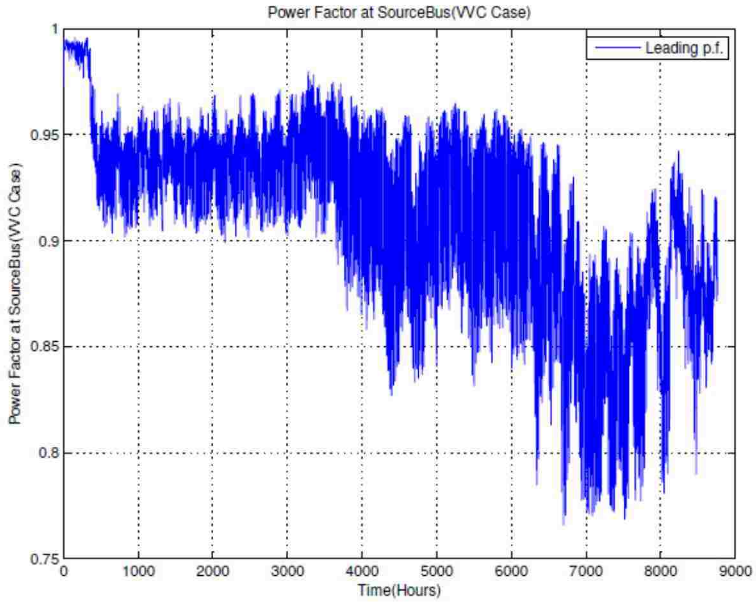

Figure 3.13: Power factor at substation, voltage regulation control case

4. COST BENEFIT ANALYSIS OF VVC CASES VERSUS BASE CASE

4.1. SYSTEM ACTIVE POWER LOSSES AND THEIR IMPORTANCE TO UTILITIES

It is evident from Figures 2.2, 3.1, and 3.13 that the unity power factor case scenario has the lowest active power losses, whereas the base case scenario has the highest active power losses in the system. This can be verified from Table 4.1. For the voltage control case, the system active power losses are in between for the voltage control case.

Apart from the responsibility of maintaining a healthy power factor and healthy voltages at distribution buses, utilities have the additional burden of keeping the system active power losses to a minimum. Each kilowatt that is produced costs money. Hence, it becomes very important to keep the active power losses in the system at its minimum.

As seen from the three case scenarios, the active power losses are minimum for the UPF case scenario, and maximum for the base case scenario. However, a comprehensive analysis is needed to determine the annual cost savings of VVC to which these losses translate.

4.2. RECOMMENDED SYSTEM SETTINGS FOR PERFORMING SIMULATION

The following are the bus settings used for all the three simulation case scenarios:

V (source) = 1.05 p.u. (base voltage of 24.9 kV)

Base MVA = 100 MVA (default)

Note that if the recommended settings are not used, it is possible that the objective of the VVC may not be accomplished, especially in the absence of voltage regulators to aid the SSTs. For example, if a source voltage of 1 p.u. is used instead of 1.05 p.u., the voltage control case scenario may not achieve the required voltage regulation of $0.95 < V_{bus} < 1.05$ p.u. at all distribution buses. Hence the use of these system settings are recommended for successful VVC.

4.3. COST BENEFIT ANALYSIS OF VVC CASES VERSUS BASE CASE

A cost benefit analysis of performing VVC with respect to the base case scenario is performed. The system active power losses for the year 2013 are recorded at each hour, for the three case scenarios. The total active power losses are obtained for both VVC cases and the base case. The cost incurred due to active power losses for each case is then calculated by multiplying the total active power losses in each case with a multiplier of 0.1$/kW (considering a cost of 10 cents/kW as the cost of production). Table 4.1 compares the total system active power losses for each of the case scenarios. The resultant cost benefit of each VVC case is obtained by subtracting the costs incurred by the losses in base case scenario, from the costs incurred by the losses in the respective VVC case scenario.

Table 4.1 Cost benefit analysis of VVC cases versus base case

Total annual losses(kW)	Base case	UPF case	Voltage regulation control case
	1466654.016	1075320.221	1396758.029
Total cost incurred on losses	$146,665.40	$107,532.02	$139,675.80
Annual cost benefit of (UPF case & voltage regulation control case) versus base case	$0.00	$39,133.38	$6,989.60

5. CONCLUSIONS

It is observed from Table 4.1 that the unity power factor case scenario of VVC offers the maximum cost advantage, while providing reasonable voltage profiles at its various distribution buses. The voltage improvement case scenario of VVC offers limited cost advantage, but provides the desired regulated voltages at all its distribution buses. Therefore, the choice of one VVC method over another is really a question of prioritization between the two power quality indicators: power factor or voltage. If a particular test case does not produce voltages as low as in the base case, then it might be beneficial to go with unity power factor solution. But cases where unacceptably low voltages occur, setting reasonable voltage regulation limits (for e.g. $0.9 < V_{bus} < 1.0$ p.u.) for voltage regulation control could offer us both a reasonable cost advantage and acceptable voltage profiles.

BIBLIOGRAPHY

[1] R. N. Allan, R. Billinton, I. Sjarief, L. Goel and K. S. So, "A reliability test system for educational purposes-basic distribution system data and results," *Power Systems, IEEE Transactions on*, vol. 6, no. 2, pp. 813-820, May 1991.

[2] R. Billinton, S. Kumar, N. Chowdhury, K. Chu, K. Debnath, L. Goel, E. Khan, P. Kos, G. Nourbakhsh and J. Oteng-Adjei, "A reliability test system for educational purposes-basic data," *Power Systems, IEEE Transactions on,* vol. 4, no. 3, pp. 1238-1244, August 1989.

[3] R. Billinton and S. Jonnavithula, "A test system for teaching overall power system reliability assessment," *Power Systems, IEEE Transactions on,* vol. 11, no. 4, pp. 1670-1676, November 1996.

[4] P. Wong, P. Albrecht, R. Allan, R. Billinton, Q. Chen, C. Fong, S. Haddad, W. Li, R. Mukerji, D. Patton, A. Schneider, M. Shahidehpour and C. Singh, "The IEEE Reliability Test System-1996. A report prepared by the Reliability Test System Task Force of the Application of Probability Methods Subcommittee," *Power Systems, IEEE Transactions on*, vol. 14, no. 3, pp. 1010-1020, August 1999.

[5] D. G. Shah and M. L. Crow, "Online Volt-Var Control for Distribution Systems With Solid State Transformers," in *Power Delivery, IEEE Transactions on*, doi: 10.1109/TPWRD.2015.2457442.

[6] IEEE PES Distribution System Analysis Subcommittee's Distribution Feeder Working Group, Distribution test feeders. [Online]. Available: http://ewh.ieee.org/soc/pes/dsacom/testfeeders/

[7] Solid-state transformers ready to enable the Smart Grid? [Online]. Available: http://www.freedm.ncsu.edu/index.php?s=2&t=news&p=121

[8] The Open Distribution System Simulator, (OpenDSS). [Online]. Available: https://sourceforge.net/p/electricdss/code/HEAD/tree/trunk/Distrib/Doc/OpenDSS Primer.pdf/

[9] Hourly Load Data Archives. [Online]. Available: http://www.ercot.com/gridinfo/load/load_hist/

[10] Power Quality Problems and New Solutions. [Online]. Available: http://www.icrepq.com/pdfs/PL4.ALMEIDA.pdf

[11] Review of Recent Developments, Solid State Transformer (SST). [Online]. Available: http://www.ripublication.com/aeee_spl/aeeev4n1spl_07.pdf

VITA

Guruprasad Ramani was born in New Delhi, India, on January 11, 1988. He finished high school in 2005. Between August 2005 and July 2009, he studied electrical engineering from Delhi Technological University, New Delhi, India and earned his bachelor's degree. He worked as an Automation and Controls Engineer with Alstom Grid in India from July 2009 to October 2013. He then moved to the United States in January 2014 to pursue his master's degree in electrical engineering. He received his master's degree in electrical engineering from Missouri University of Science and Technology in May 2016.